

PAPER • OPEN ACCESS

Synthesis and Crystal Structure Analysis of $\text{LiNiSi}_x\text{P}_{1-x}\text{O}_4/\text{C}$ as a Cathode Material for the Lithium-ion Batteries Application

To cite this article: A A Fibriyanti *et al* 2019 *IOP Conf. Ser.: Mater. Sci. Eng.* **515** 012043

View the [article online](#) for updates and enhancements.

Synthesis and Crystal Structure Analysis of $\text{LiNiSi}_x\text{P}_{1-x}\text{O}_4/\text{C}$ as a Cathode Material for the Lithium-ion Batteries Application

A A Fibriyanti¹, A Fuad^{1,2}, W Astutik¹, N Hidayat^{1,2}, B Prihandoko³, N Mufti^{1,2}, M Diantoro^{1,2,*}

¹ Department of Physics, Faculty of Mathematics and Natural Sciences, Universitas Negeri Malang, Jl. Semarang 5, Malang 65145, East Java, Indonesia

² Center of Advanced Materials for Renewable Energy (CAMRY), Universitas Negeri Malang, Jl. Semarang 5, Malang 65145, East Java, Indonesia

³ Research Center for Physics- LIPI, PUSPITEK, Tangerang Selatan, Indonesia

*Corresponding author's email: markus.diantoro.fmipa@um.ac.id

Abstract. Lithium-ion batteries are currently the most promising storage device. An electronic conductivity is a key factor that affects the performance of Lithium-ion batteries (LiB). In this work, $\text{LiNiSi}_x\text{P}_{1-x}\text{O}_4/\text{C}$, ($x = 0.00, 0.05, 0.10, 0.15, \text{ and } 0.20$) as cathode materials were effectively synthesized by a solid-state reaction technique. To enhance the ionic conductivity of Lithium-Ion Battery application, we used sucrose as a carbon source and Si ion as a dopant in LiNiPO_4 cathode material. The effect of Si dopant on its crystal structure, composition, and functional groups existing in cathode material $\text{LiNiSi}_x\text{P}_{1-x}\text{O}_4/\text{C}$ are investigated analytically. The samples were characterized by using the X-ray Diffractometer (XRD), X-Ray fluorescence (XRF), and Fourier Transform Infrared Spectroscopy (FTIR). The different amount of Si dopant promotes the structural modification and important role to improve the rate performance of LiB.

Keywords: Crystal structure, cathode, $\text{LiNiSi}_x\text{P}_{1-x}\text{O}_4/\text{C}$, lithium-ion battery

1. Introduction

Energy storage, such as batteries and supercapacitors, is a component to produce a sustainable energy system [1]. The development was influenced by several factors including the active constituent material which can affect its electrical and dielectric properties [2,3]. At this time, one of the rechargeable batteries that attracted the most attention of researchers is Lithium-ion Batteries (LiB). LiB technology has been widely developed in various electronic devices over the past 20 years [4] and intensively applied to Hybrid Electric Vehicles (HEV), Plug-in Hybrid Electric Vehicles (PHEV), and Electric Vehicles (EV) [5]. LiB component consists of cathode, anode, electrolyte, and separator material [6]. One component plays an important role in improving the quality of the battery is a cathode. The cathode is a positive electrode that acts as an electric current when the charging and emptying process occurs in the battery. The cathode material with Olivine phosphate structure is very interesting and specifically it has been studied as cathode LiB material with a high potential energy, abundance in nature, low toxicity, environmentally friendly, has good electrochemical performance that is stable when overloading and has good thermal stability during charging and discharging processes [7,8]. In the group olivine orthophosphates structure LiMPO_4 ($M = \text{Fe, Mn, Co, and Ni}$), LiCoO_2 and LiFePO_4 are currently the



cathode material most widely used in commercial LiB because they have a good life cycle (> 500 cycles) [9]. Air stability of LiCoO_2 cathode material is high and able to be produced on a large scale. However, it requires high production costs and has high cobalt toxicity. While the LiFePO_4 cathode material includes environmentally friendly materials with low production costs and has good air stability and life cycle. However, the capacity is relatively low which is theoretically 170 mAh/g [10].

Based on the research of Cheruku *et al.*, LiMnPO_4 has the highest ionic conductivity compared to other types of olivine phosphate materials structure due to weak Li-O bonds resulting from the largest unit cell volume [11]. However, among the four types of lithium phosphate transition metals with olivine structures, LiNiPO_4 has the highest operational voltage of $\sim 5.1 \text{ V vs. Li / Li}^+$ and specific energy density of about 800 Wh/kg [12]. The main advantage of LiNiPO_4 is its high stability, is inexpensive and environmentally friendly. However, the electronic and ionic conductivity like another olivine structure cathode materials is insufficiently high. This condition allows to reduce a specific capacity during a high-speed discharge. Many efforts have been made to improve the electrochemical performance and eventually to improve electrical properties by manipulating the active materials through the addition of carbon additives to the olivine matrix, coating the surface of particles with a thin layer of carbon, or reducing particle size [13].

In this study, LiNiPO_4 cathode material was synthesized by doping Si element into P and Carbon coating (C) with the chemical equation $\text{LiNiSi}_x\text{P}_{1-x}\text{O}_4/\text{C}$ using a solid-state reaction method. Here, microstructure analysis of cathode material was carried out to provide a good understanding of the synthesis of cathode $\text{LiNiSi}_x\text{P}_{1-x}\text{O}_4/\text{C}$ material to improve the performance of electrochemical properties in LiB.

2. Methods

The synthesis of cathode material $\text{LiNiSi}_x\text{P}_{1-x}\text{O}_4/\text{C}$ ($x = 0 \leq 0.2$) was carried out in two stages, namely the synthesis of $\text{LiNiSi}_x\text{P}_{1-x}\text{O}_4$ and carbon coating (C) on the prepared $\text{LiNiSi}_x\text{P}_{1-x}\text{O}_4$. The $\text{LiNiSi}_x\text{P}_{1-x}\text{O}_4$ material was prepared using are precursor consisting of powder $\text{LiOH}\cdot\text{H}_2\text{O}$, Ni, and $\text{SiO}_2\cdot\text{H}_2\text{O}$ which are mixed and ground in a mortar to be a homogeneous mixture, and then added a certain amount of H_3PO_4 as a solvent. The process was continued by heating the mixture in the oven and refining it after drying. Calcination was carried out at $700 \text{ }^\circ\text{C}$ for 2 hours in an inert gas. The calcined material is then smoothed using a ball-milling tool for 2 hours. The sample was sintered at $900 \text{ }^\circ\text{C}$ for 6 hours. The sintered product was pulverized and followed by sieving with a 400 mesh. The carbon coating process was carried out by adding sucrose ($\text{C}_{12}\text{H}_{22}\text{O}_{11}$) into $\text{LiNiSi}_x\text{P}_{1-x}\text{O}_4$ powder with a ratio of 1: 1. The mixture was then ground using a mortar. The coating process was performed by heating the mixture at $700 \text{ }^\circ\text{C}$ for 20 minutes. We characterized the material FTIR, X-RD, and SEM to determine the functional group, crystal structure, and their morphology.

3. Results and Discussions

Figures 1 (a) and (b) show the spectra of functional group bonds from the FTIR $\text{LiNiSi}_x\text{P}_{1-x}\text{O}_4$ and $\text{LiNiSi}_x\text{P}_{1-x}\text{O}_4/\text{C}$. Figure 1a shows that in each sample the absorbance peak of the functional group $\text{LiNiSi}_x\text{P}_{1-x}\text{O}_4$ appears in the range of wave numbers $\sim 1147\text{-}1149$ (ν_3 (PO_4) stretching), $\sim 1095\text{-}1097$ is (ν_3 (PO_4) stretching), ~ 943 (ν_1 (PO_4) stretching), $\sim 648\text{-}651$ (ν_4 (PO_4) bending), $\sim 573\text{-}584$ (ν_2 (PO_4) bending), $\sim 547\text{-}551$ (Ni-O), and $\sim 433\text{-}482$ (Li-O) cm^{-1} [8,11]. For Si-doped samples, the Si-O at wave peak appears at a number $\sim 748\text{-}817 \text{ cm}^{-1}$ [14]. The existing of the main peaks showing that the $\text{LiNiSi}_x\text{P}_{1-x}\text{O}_4$ sample has been successfully formed. Figure 1b shows similar spectra such as the samples without carbon coating. However, there is another absorbance peak, namely C = C located at a wave number $\sim 1593\text{-}1596 \text{ cm}^{-1}$ [5]. This shows that carbon coatings have been successfully carried out.

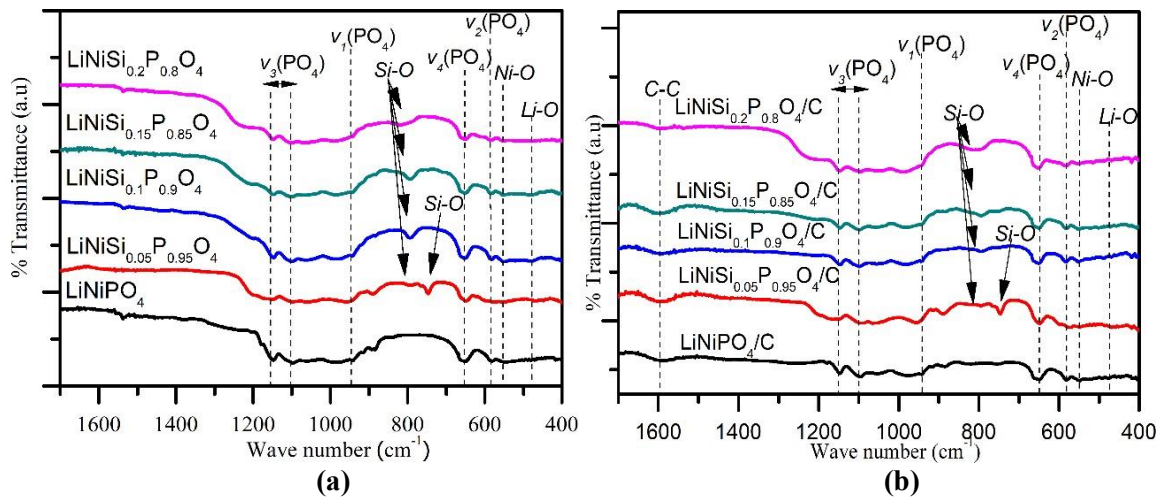


Figure 1. FTIR spectrum of (a) $\text{LiNiSi}_x\text{P}_{1-x}\text{O}_4$, and (b) $\text{LiNiSi}_x\text{P}_{1-x}\text{O}_4/\text{C}$

Figure 2 shows the XRD patterns of the $\text{LiNiSi}_x\text{P}_{1-x}\text{O}_4/\text{C}$ sample using the solid-state reaction method. By using X'pert High Score Plus software, we found that the diffraction peaks express the existing an orthorhombic crystal structure under the $Pnma$ space group. The main diffraction peaks of (020), (011), (111), (200), (131), (222) associated to 2θ at 17.72° , 20.99° , 25.97° , 30.53° , 36.42° , and 53.33° respectively according to the JCPDS card no. 01-088-1297. The absence of silicon (Si) diffraction peaks detected in each sample indicated that Si successfully replaces P site in the structure. The Si doping did not form a new phase in $\text{LiNiSi}_x\text{P}_{1-x}\text{O}_4/\text{C}$. We found also no carbon diffraction peak. It indicates that the carbon in the sample is amorphous. However, it can be seen in Figure 2 that a new phase diffraction peak is detected around the $2\theta = 22.4^\circ$, 34.0° , dan 43.5° . Based on research conducted by Minakashi et al., 2011, the diffraction peak is Li_3PO_4 (22.4° , 34.0°) and NiO (43.5°) [15]. Accordingly, the Lithium Nickel Phosphate phase produced in this study contained the impurity of Li_3PO_4 and NiO .

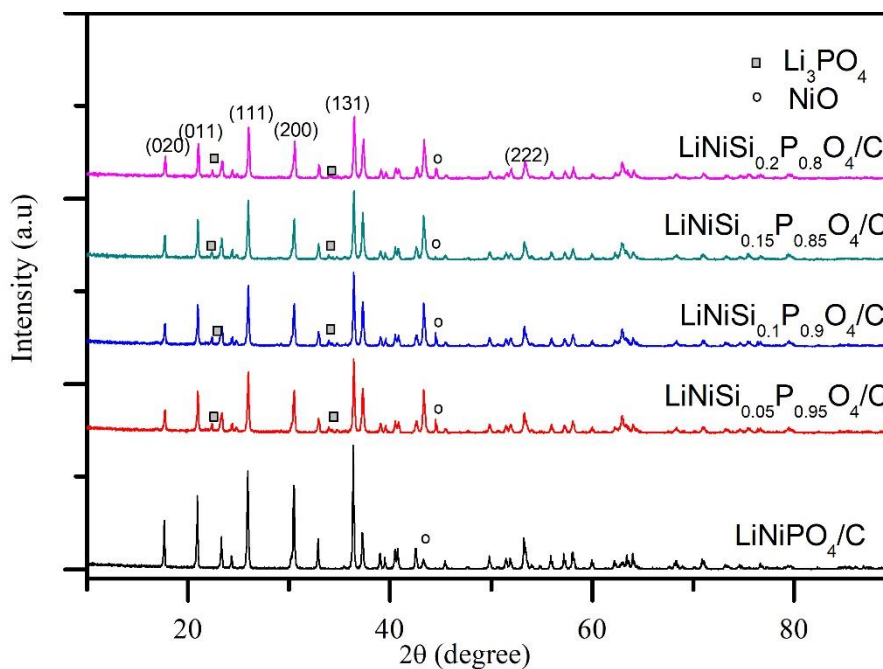


Figure 2. XRD Pattern of $\text{LiNiSi}_x\text{P}_{1-x}\text{O}_4/\text{C}$

The existence of the impurity phase is possible due to the calcination at a temperature of ~ 800 °C [13]. On the other hand, to identify the success of doping the Si element into P, the analysis was carried out as shown in Figure. 3. It shows the diffraction peaks of $\text{LiNiSi}_x\text{P}_{1-x}\text{O}_4/\text{C}$ at (111) planes shifted toward a smaller angle. The (111) diffraction planes of each sample with increasing Si doping sequentially are located at 2θ of 25.97° , 25.95° , 25.94° , 25.92° and 25.90° . This shift indicates that Si successfully entered into the $\text{LiNiSi}_x\text{P}_{1-x}\text{O}_4/\text{C}$ crystal lattice [16].

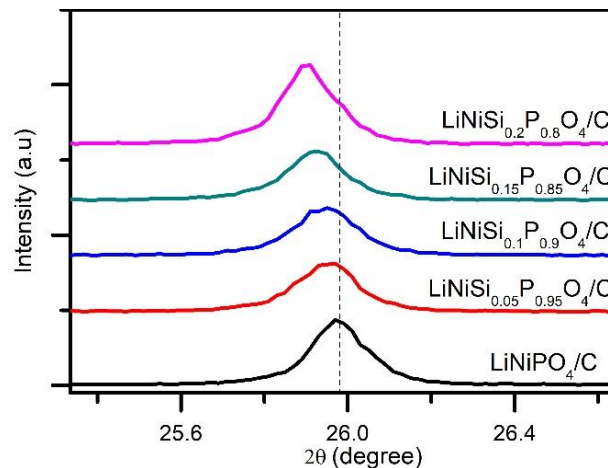


Figure 3. Peak shift of $\text{LiNiSi}_x\text{P}_{1-x}\text{O}_4/\text{C}$

Table 1. Crystal Structure of $\text{LiNiSi}_x\text{P}_{1-x}\text{O}_4/\text{C}$

| Sample | Parameter | | | | | | |
|--|-----------|---------|---------|-----------------|-------|-------|----------|
| | a (Å) | b (Å) | c (Å) | $V(\text{Å}^3)$ | GoF | R_p | R_{wp} |
| LiNiPO_4/C | 10.0355 | 5.8586 | 4.6792 | 275.1128 | 1.71 | 15.67 | 21.45 |
| $\text{LiNiSi}_{0.05}\text{P}_{0.95}\text{O}_4/\text{C}$ | 10.0352 | 5.8614 | 4.6795 | 275.2508 | 1.67 | 14.95 | 21.46 |
| $\text{LiNiSi}_{0.1}\text{P}_{0.9}\text{O}_4/\text{C}$ | 10.0329 | 5.8626 | 4.6798 | 275.2606 | 1.83 | 16.22 | 23.26 |
| $\text{LiNiSi}_{0.15}\text{P}_{0.85}\text{O}_4/\text{C}$ | 10.0371 | 5.8654 | 4.6806 | 275.5554 | 1.68 | 16.21 | 22.79 |
| $\text{LiNiSi}_{0.2}\text{P}_{0.8}\text{O}_4/\text{C}$ | 10.0399 | 5.8677 | 4.6819 | 275.8194 | 1.78 | 16.25 | 23.02 |

The crystal structure of $\text{LiNiSi}_x\text{P}_{1-x}\text{O}_4/\text{C}$ can be determined through analysis using Rietica program. The obtained crystal structure parameters are shown in Table 1. It indicates that the addition of Si doping affects the lattice parameter. The lattice parameter increases with increasing of Si, so the crystal volume increases too. This can increase the diffusion rate of Li ions during the intercalation process. The crystal size was calculated using the *Scherrer formula*, the results obtained are shown in Table 2.

Table 2. Crystal size of $\text{LiNiSi}_x\text{P}_{1-x}\text{O}_4/\text{C}$

| Sample | Crystal Size (nm) |
|--|-------------------|
| LiNiPO_4/C | 49.52 |
| $\text{LiNiSi}_{0.05}\text{P}_{0.95}\text{O}_4/\text{C}$ | 47.01 |
| $\text{LiNiSi}_{0.1}\text{P}_{0.9}\text{O}_4/\text{C}$ | 43.92 |
| $\text{LiNiSi}_{0.15}\text{P}_{0.85}\text{O}_4/\text{C}$ | 42.85 |
| $\text{LiNiSi}_{0.2}\text{P}_{0.8}\text{O}_4/\text{C}$ | 43.38 |

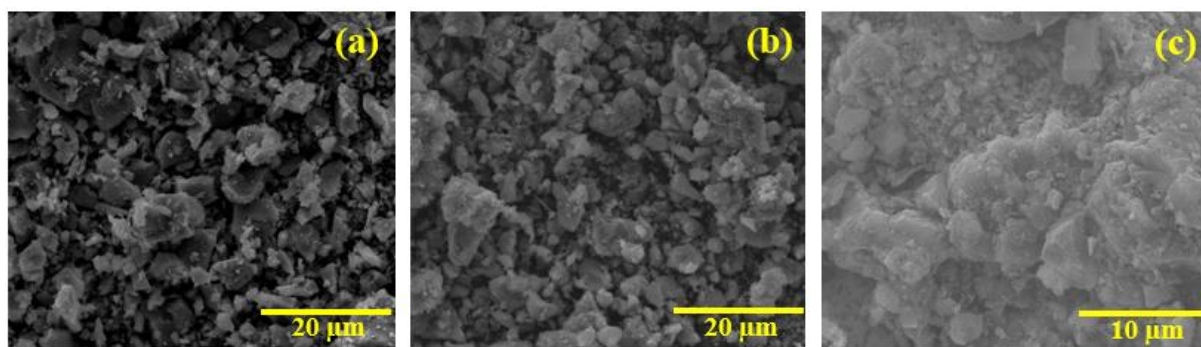


Figure 4. SEM result of (a) LiNiPO_4 , (b) $\text{LiNiSi}_{0.1}\text{P}_{0.9}\text{O}_4$ dan (c) $\text{LiNiSi}_{0.1}\text{P}_{0.9}\text{O}_4/\text{C}$

From the SEMs images, we calculated the particle sizes using ImageJ software. As seen in Figure 4a, and 4b, we found that the crystal size is $1.05 \mu\text{m}$ and $1.17 \mu\text{m}$, respectively. As for Figure 4c, the $\text{LiNiSi}_{0.1}\text{P}_{0.9}\text{O}_4/\text{C}$ material obtained an average particle size of $0.65 \mu\text{m}$. This explains that the presence of Si doping increases the particle size. On the other hand, the presence of carbon coatings can cause particle size to decrease.

4. Conclusion

The $\text{LiNiSi}_x\text{P}_{1-x}\text{O}_4/\text{C}$ cathode material has been successfully fabricated. The functional groups, as well as crystal structure analyses, support the appearance of the phases. The material has an orthorhombic crystal structure. The presence of Si doping gives rise to increase their lattice parameter so crystal volume. The substitution of Si in the P site increases the grain size. The carbon coating, in contrast to Si doping, reduces the particle size.

References

- [1] Mustikasari A A, Diantoro M, Mufti N and Suryana R 2018 The Effect of Nano ZnO Morphology on Structure, Dielectric Constant, and Dissipation Factor of Ca-Nano ZnO/ITO Films *J. Neutrino* **10** 65
- [2] Diantoro M, Hidayati N N S, Latifah R, Fuad A, Nasikhudin, Sujito and Hidayat A 2016 Electrical conductivity modification using silver nano particles of *Jatropha Multifida L.* and *Pterocarpus Indicus w.* extracts films *AIP Conf. Proc.* **1719** 1–8
- [3] Diantoro M, Mustikasari A A, Wijayanti N, Yogihati C and Taufiq A 2017 Microstructure and dielectric properties of cellulose acetate-ZnO/ITO composite films based on water hyacinth *J. Phys. Conf. Ser.* **853** 0–9
- [4] Xu B, Qian D, Wang Z and Meng Y S 2012 Recent progress in cathode materials research for advanced lithium ion batteries **73** 51–65
- [5] Muraliganth T, Stroukoff K R and Manthiram A 2010 Microwave-Solvothermal Synthesis of Nanostructured $\text{Li}_2\text{MSiO}_4/\text{C}$ (M = Mn and Fe) Cathodes for Lithium-Ion Batteries 5754–61
- [6] Deng D 2015 ion batteries : basics , progress , and challenges
- [7] Armand M 2001 Issues and challenges facing rechargeable lithium batteries **414** 359–67
- [8] Karthickprabhu S, Hirankumar G, Maheswaran A, Sanjeeviraja C and Bella R S D 2013 Structural and conductivity studies on LiNiPO_4 synthesized by the polyol method *J. Alloys Compd.* **548** 65–9
- [9] Chung S Y, Bloking J T and Chiang Y M 2002 Electronically conductive phospho-olivines as lithium storage electrodes *Nat. Mater.* **1** 123–8
- [10] Masquelier C, Padhi A K, Nanjundaswamy K S and Goodenough J B 1998 New Cathode Materials for Rechargeable Lithium Batteries: The 3-D Framework Structures $\text{Li}_3\text{Fe}_2(\text{XO}_4)_3$ (X = P,As) **234** 228–34
- [11] Cheruku R, Kruthika G, Govindaraj G and Vijayan L 2015 Journal of Physics and Chemistry of

- Solids Electrical relaxation studies of olivine type nanocrystalline LiMPO_4 (M = Ni, Mn and Co) materials *J. Phys. Chem. Solids* **86** 27–35
- [12] Dimesso L, Spanheimer C and Jaegermann W 2012 *Solid State Sciences* **14** 1372–7
- [13] Zaghbi K, Mauger A and Julien C M 2015 *Olivine-Based Cathode Materials*
- [14] Karakassides M A 1999 An Infrared Reflectance Study of Si-O Vibrations in Thermally Treated Alkali-Saturated Montmorillonites *Clay Miner.* **34** 429–38
- [15] Minakshi M, Singh P, Appadoo D and Martin D E 2011 Synthesis and characterization of olivine LiNiPO_4 for aqueous rechargeable battery *Electrochim. Acta* **56** 4356–60
- [16] Zhao J, Zhao S, Wu X, Cheng H and Nan C 2017 Double role of silicon in improving the rate performance of LiFePO_4 cathode materials *J. Alloys Compd.* **699** 849–55

Acknowledgements

We would like to thank Universitas Negeri Malang for providing us with PNBPN 2018 research grant.